International Journal of the Physical Sciences Vol. 6(11), pp. 2701-2709, 4 June, 2011
Available online at http://www.academicjournals.org/IJPS
DOI: 10.5897/IJPS11.540
ISSN 1992 - 1950 ©2011 Academic Journals

Full Length Research Paper

A visual inspection system for quality control of optical lenses

Hong-Dar Lin*, Yuan-Shyi Peter Chiu and Shih-Yin Hsu

Department of Industrial Engineering and Management, Chaoyang University of Technology, 168 Jifong E. Road, Wufong District, Taichung 41349, Taiwan.

Accepted 3 May, 2011

This paper proposes a quality inspection system for optical lenses using computer vision techniques. The system is able to inspect LED (Light-Emitting Diode) lenses visually and to validate their quality level automatically based on the defect severity. The optical inspection system applies the block discrete cosine transform (BDCT), Hotelling T^2 statistic, and grey clustering technique to detect visual defects of LED lenses. A spatial domain image with equal sized blocks is converted to DCT (Discrete Cosine Transform) domain and some representative energy features of each DCT block are extracted. These energy features of each block are integrated by the T^2 statistic and the suspected defect blocks can be determined by the multivariate statistical method. Then, the grey clustering algorithm based on the block grey relational grades is conducted to further confirm the block locations of real defects. Finally, a simple segmentation method is applied to set a threshold for distinguishing between defective areas and uniform regions. Experimental results show the defect detection rate of the proposed method is 94.64% better than those of traditional spatial and frequency domain techniques.

Key words: Industrial engineering, quality inspection, optical lens, visual defect, computer vision system.

INTRODUCTION

A lens is an optical device with perfect or approximate axial symmetry which transmits and refracts light, converging or diverging the beam. Lenses are typically made of glass or transparent plastic. Optical lenses are transparent components made from optical-quality materials and curved to converge or diverge transmitted rays from an object. These rays then form a real or virtual image of the object. There are many types of optical lenses. Optical lenses are widely used in cell phone, notebooks, automotive, digital camera, scanner, LED (Light-Emitting Diode) etc.

An LED is a semiconductor device that emits visible light when an electric current passes through the semiconductor chip. Compared with incandescent and fluorescent illuminating devices, LEDs have lower power requirement, higher efficiency, and longer lifetime. Typical applications of LED components include indicator lights, LCD (Liquid Crystal Display) panel backlighting, fiber optic data transmission, etc. To meet consumer and industry needs, LED products are being made in smaller sizes, which increase difficulties of product inspection. The functions of LED lenses include focusing, beauty, and protection to avoid the waste of light and light pollution. An LED without the assistance of lens focus function cannot project light to the intended location. Therefore, LED lenses are invented to improve the light scattering problems of LEDs and they are widely applied to hand flashlights and traffic lights applications. Figure 1 shows the common LED lenses and the basic LED lens structure diagram.

Lens inspection requires special physical conditions, particularly in terms of lighting. In the real working situation, each inspected lens is brought into the inspector's field of vision. The lenses are round and transparent; the defect to be inspected could be located on the external surface of the lenses or inside. A lens presents a certain thickness and a certain curvature, both of which vary. At times, lenses provide the same perceptive result as a magnifying glass, and the defects

*Corresponding author. E-mail: hdlin@cyut.edu.tw Tel: 886-4-2332-3000, Ext. 4258. Fax: 886-4-2374-2327.

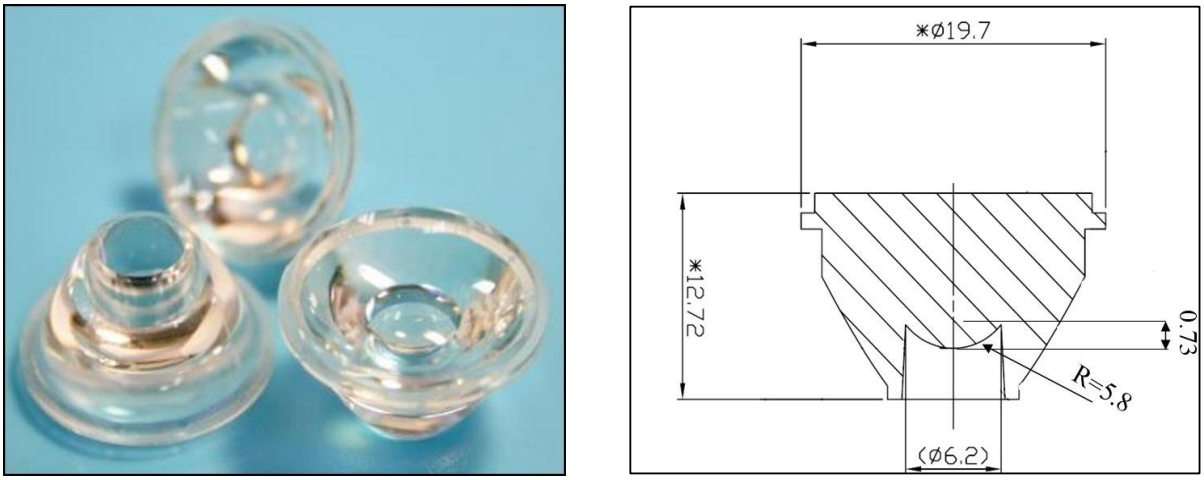

Figure 1. (a) LED lenses, and (b) LED lens structure diagram.

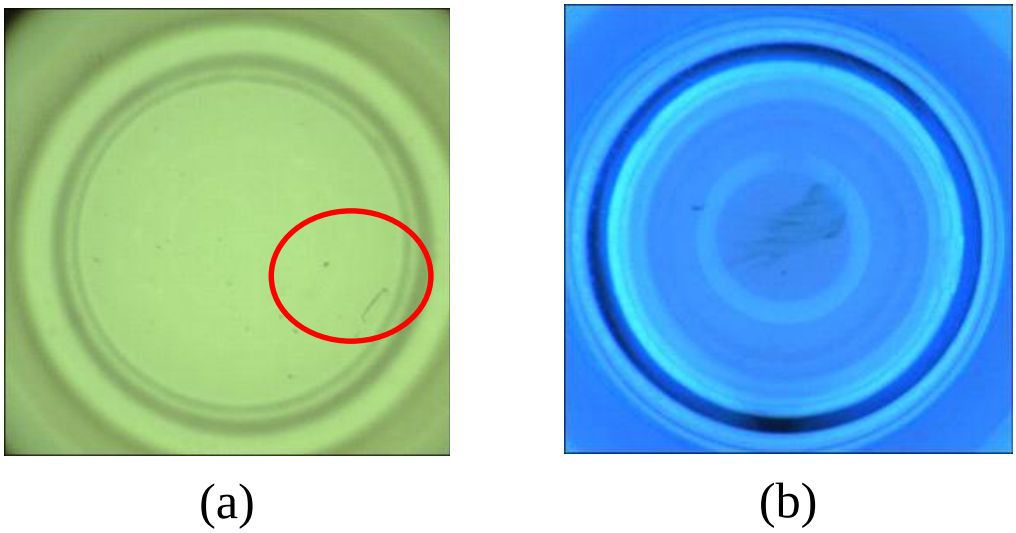

Figure 2. LED lenses with visual defects (from top view) (a) LED lens with scratch and pinhole defects; (b) LED lens with dirt defects a period.

are all the more difficult to track down and to locate in the area of the lens. The majority of defects are not only very small but also they are extremely diverse and can assume various forms. Figure 2 presents LED lenses with visual defects.

Currently, the most common detection methods for LED lens defects are human visual inspection. Human visual inspection is tedious, time-consuming and highly dependent on the inspectors' experiences, conditions, or moods. Erroneous judgments are easily made because of inspectors' subjectivity and eye fatigues. Difficulties exist in precisely inspecting tiny flaws by machine vision systems because when product images are being captured, the area of a tiny flaw could expand, shrink or even disappear due to uneven illumination of the environment, transparent and curved surfaces of the product, and so on. Seeing the great need for an automated visual detection scheme for LED lens defects, we propose a block discrete cosine transform (BDCT) based approach to overcome the difficulties of traditional machine vision systems.

Inspection of surface defects has become a critical task for manufacturers who strive to improve product quality and production efficiency. Defect detection techniques, generally classified into the spatial domain and the frequency domain, compute a set of textural features in a

sliding window and search for significant local deviations among the feature values. Latif-Amet et al. (2000) presented wavelet theory and co-occurrence matrices for detection of defects encountered in textile images and classify each sub-window as defective or non-defective with a Mahalanobis distance. Cho et al. (2005) applied the adaptive threshold technique and morphology method to detect defects from images of uniform fabrics for developing a real-time vision system.

As to techniques in the frequency domain, Chan and Pang (2000) used the Fourier transform to detect fabric defects. Tsai and Hsiao (2001) proposed a wavelet transform based approach for inspecting local defects embedded in homogeneous textured surfaces. By properly selecting the smooth sub-image or the combination of detail sub-images in different decomposition levels for backward wavelet transform, regular, repetitive texture patterns can be removed and only local anomalies are enhanced in the reconstructed image. Also, Lin and Ho (2007) developed a novel approach that applies discrete cosine transform based enhancement for the detection of pinhole defects on passive component chips.

As to inspecting defects of lenses, Rebsamen et al. (2010) described quality control tasks in the optical industry from a work analysis of optical lens inspection to a training program. Martinez et al. (2009) developed a vision sensor planning system for automated inspection of headlamp lenses. This system uses the lens CAD (Computer Aided Design), a vision sensor model and the customer requirements describing by a fuzzy approach, to achieve an optimal set of viewpoints by genetic algorithm. Bazin et al. (2006) proposed a novel method for the industrial inspection of ophthalmic contact lenses in a time constrained production line environment. Perng et al. (2010) presented a new inspection system that uses machine vision to detect optical defects in quasi-contact lenses. The optical region of the lens image is first segmented, and then the middle axes of each fringe on the optical region are determined. Three features of the fringe are extracted to create a mapping of the original features to a semantic description of the textures. Finally, the quality of the quasi-contact lens is determined by a control chart procedure. Therefore, most of the existing researches focus on inspections of optical lenses, headlamp lenses, and contact lenses. They do not detect defects with the properties of tiny defects on LED lenses. Consequently, we present a new approach using block discrete cosine transform and grey clustering for defect detection of the transparent and curved LED lens surfaces.

Grey system proposed by Deng (1989) means that the information within a system is partially unknown. Grey theory provides the applications of clustering analysis, relational analysis, predication, and decision for the grey system. The grey theory has the advantage of being able to deal with complex problems involving uncertain or incomplete systems. Grey clustering is a common grey theory application, which classifies unknown samples into specified groups by comprehensively integrating the various attribute intensities of each sample (Tsai et al., 2006). Heng (2010) analyzed infrared images based on grey system and applied grey clustering to filter out possible objects for detecting infrared targets. Huang (2008) employed image processing techniques and a modified unsupervised grey clustering algorithm to estimate the location of each die and identify the spot number accurately and effectively. Lin et al. (2009) proposed a method for incipient fault diagnosis in oil-immersed transformers using grey clustering analysis. Their method could avoid the determination of the linguistic variables, membership functions, inference rules, network architecture, and parameters assignment, and is easy to implement in the portable device.

Hu et al. (2002) proposed a grey clustering method incorporating the grey relational grades into learning rules of self-organizing feature maps for solving classification and traveling salesman problems. Lin and Lee (2009) developed an improved model integrating grey number into grey clustering technique to deal with the evaluation problems under the condition of insufficient and uncertain information. Tsai et al. (2006) used grey clustering operation for color image evaluation in product form and color design. Madhuri and Chandulal (2010) combined grey relational analysis and grey clustering to evaluate the website for providing useful information for users and estimating the validation and popularity of the websites. Therefore, grey clustering technique has been successfully applied in the fields of engineering detection, classification, decision-making, product design, performance evaluation, etc. in recent years.

METHODS

By regarding an input image as a matrix, we can perform the DCT transformation to transform a spatial domain image into the frequency domain. A spatial domain image with equal sized blocks is converted to DCT domain and some representative energy features of each DCT block are extracted. These energy features of each block are integrated by the T^2 statistic and the suspected defect blocks can be determined by the multivariate statistical method. Then, the grey clustering algorithm based on block grey relational grades is conducted to further confirm the block locations of real defects. Finally, a simple segmentation method is applied to set a threshold for distinguishing between defective areas and uniform regions. Therefore, the visual defects on the curved surfaces of LED lenses can be accurately detected and located by the proposed method.

Block discrete cosine transform

The inspection task of this paper involves detecting novel but obscurely faulty items, visual defects on LED lenses of optical components. Many of these unanticipated defects are extremely small in size and can not be described by explicit measures, thus making automated defect detection difficult. Since DCT has the advantages of packing the most information into the fewest

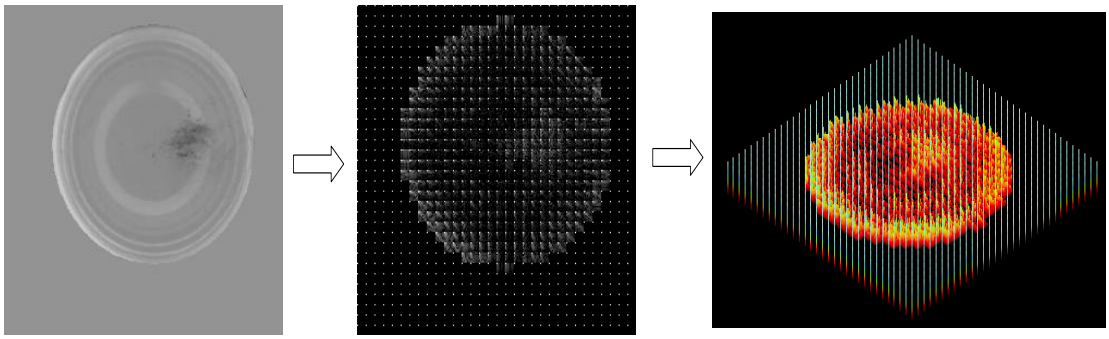

Figure 3. Examples of the BDCT transformation (a) an LED lens image with visual defects; (b) the 2-D BDCT spectrum image, and (c) the power spectra in 3-D perspective.

coefficients and minimizing reconstruction errors, only a small amount of information of a detailed image will be lost during the image processing procedures (Gonzalez and Woods, 2008). Such advantages make DCT suitable and favorable for our study of visual defect detection of optical components. To increase the computational efficiency of DCT, the BDCT is adopted that we divide an image into non-overlapping image blocks of equal size which can be conducted DCT individually instead of taking one transform on an entire image.

Ahmed et al. (1974) first defined DCT as one-dimensional (1-D) and suitable for 1-D digital signal processing. Equation (1) gives the expression for computing the BDCT of a digital image $d_{x,y}$ of block size $P \times Q$. This expression must be computed for all values of u = 0, 1, 2, …, P-1, and also for all values of v = 0, 1, 2, …, Q-1. While u and v are frequency variables, x and y are spatial variables.

$$D_{u,v} = \rho(u)\rho(v)\sum_{x=0}^{P-1}\sum_{y=0}^{Q-1} d_{x,y}\cos\left[\frac{(2x+1)u\pi}{2P}\right]\cos\left[\frac{(2y+1)v\pi}{2Q}\right] \quad (1)$$

where

$$\rho(u)=\begin{cases}\sqrt{\frac{1}{P}}, & u=0\\ \sqrt{\frac{2}{P}}, & u=1,2,3,...,P-1\end{cases}, \quad \rho(v)=\begin{cases}\sqrt{\frac{1}{Q}}, & v=0\\ \sqrt{\frac{2}{Q}}, & v=1,2,3,...,Q-1\end{cases}, \quad \begin{cases}u=0,1,2,3,...,P-1\\ v=0,1,2,3,...,Q-1\\ x=0,1,2,3,...,P-1\\ y=0,1,2,3,...,Q-1\end{cases}.$$

The power spectrum $P(u, v)$ of image $d_{x,y}$ is defined as:

$$P(u,v) = \left|D_{u,v}\right|^2 \quad (2)$$

That is, the sum of the squares of the DCT coefficients is the energy of the block.

As the origin of the BDCT coefficients has a very huge frequency component, it is sometimes called the direct current (DC) component of the BDCT frequency domain, while other coefficients are called the alternating current (AC) components. The DC coefficients in the upper left corner reflect information of lower frequencies, whereas the AC coefficients in the lower right corner reflect that of higher frequencies. BDCT has the property of concentrating the dominant energy of a typical image in the low-frequency components. This means that the coefficients of the high-frequency components are close to zero, and therefore negligible in most cases (Gonzalez and Woods, 2008).

The 2-D and 3-D BDCT spectrum diagrams of an LED lens image in Figures 3a, b and c show that a lot of energy concentrates in the origin ($u = 0, v = 0$) and that the energy decreases gradually from the origin and the low frequency zone on the top-left side to the high frequency zone on the bottom-right side. In the BDCT domain, the tiny and low-contrast defects are not only significantly enhanced but also the gradually changing intensity levels of defects are removed.

The edge pattern in a block can be fully captured from its DCT coefficients in frequency domain (Pan, 2002). The energy distribution in the DCT domain determines the edge patterns in the spatial block. One way of determining the features in the spatial block is by looking into the energy distribution in the 2D-DCT domain (Rao and Hwang, 1996). The energy concentrated in top horizontal region represents vertical edges in the block; the energy concentrated in left vertical region indicates horizontal edges in the block, and the energy concentrated in diagonal region implies diagonal edges in the block.

Five energy features of a BDCT are expressed as follows:

$$E_H = \left[\sum_{u=0}^{P-1}\sum_{v=0}^{Q-1}(v+1)^2 \times D_{u,v}^2\right]^{1/2} \qquad u+v \neq 0 \quad (3)$$

$$E_V = \left[\sum_{u=0}^{P-1}\sum_{v=0}^{Q-1}(u+1)^2 \times D_{u,v}^2\right]^{1/2} \qquad u+v \neq 0 \quad (4)$$

$$E_D = \left[\sum_{u=0}^{P-1}\sum_{v=0}^{Q-1}(u+1)\times(v+1) \times D_{u,v}^2\right]^{1/2} \qquad u+v \neq 0 \quad (5)$$

$$E_M = \frac{1}{P\times Q}\sum_{u=0}^{P-1}\sum_{v=0}^{Q-1} D_{u,v} \quad (6)$$

$$E_S = \frac{1}{(P\times Q)\text{-}1}\sum_{u=0}^{P-1}\sum_{v=0}^{Q-1}\left(D_{u,v} - E_M\right)^2 \quad (7)$$

where $P \times Q$ is the block size of BDCT, D is frequency components of BDCT, u and v are frequency coordinates of BDCT, E_H is the horizontal energy value of a BDCT, E_V is the vertical energy value of a BDCT, E_D is the diagonal energy value of a BDCT, E_M is

the average energy value of a BDCT, and E_S is the standard deviation of energy values of a BDCT.

Multivariate T^2 statistic

The five energy features extracted from a BDCT will be treated as five quality characteristics for multivariate statistical analysis. Normal texture images can be used to estimate the parameters of standard texture characteristics. The sample mean matrix ($\overline{X}$) and the sample covariance matrix (*S*) describe the properties of and the relations between the image characteristics of normal and defect images. The covariance is a measure of the relationship between two random variables. Since the five energy features do not follow a multivariate normal distribution, a logarithmic transformation ($\log_{10}$) is conducted to transform the multivariate data to be normally distributed. The probability plot can be used to determine whether sample data conform to normal distributions (Montgomery and Runger, 2007). Therefore, the sample covariance matrix (S) of a normal image can be expressed as:

$$S = \begin{bmatrix} S^2_{E_H} & S_{E_H E_V} & S_{E_H E_D} & S_{E_H E_M} & S_{E_H E_S} \\ S_{E_H E_V} & S^2_{E_V} & S_{E_V E_D} & S_{E_D E_M} & S_{E_V E_S} \\ S_{E_H E_D} & S_{E_V E_D} & S^2_{E_D} & S_{E_D E_M} & S_{E_D E_S} \\ S_{E_H E_M} & S_{E_D E_M} & S_{E_D E_M} & S^2_{E_M} & S_{E_M E_S} \\ S_{E_H E_S} & S_{E_V E_S} & S_{E_D E_S} & S_{E_M E_S} & S^2_{E_S} \end{bmatrix}_{5\times 5} \quad (8)$$

where S_p^2 is the sample variance of the *p* characteristic of a normal image, S_{pq} is the sample covariance of the *p* and *q* characteristics of a normal image. The sample mean matrix ($\overline{\mathrm{X}}$) of a normal image can be defined as:

$$\overline{X_i} = \begin{bmatrix} \overline{X_1} \\ \overline{X_2} \\ \overline{X_3} \\ \overline{X_4} \\ \overline{X_5} \end{bmatrix}_{5\times 1} = \begin{bmatrix} \log_{10}\overline{E_H} \\ \log_{10}\overline{E_V} \\ \log_{10}\overline{E_D} \\ \log_{10}\overline{E_m} \\ \log_{10}\overline{E_s} \end{bmatrix}_{5\times 1} \quad (9)$$

where
$\overline{E_H}$: average of block horizontal energy values
$\overline{E_{\mathrm{V}}}$: average of block vertical energy values
$\overline{E_{\mathrm{D}}}$: average of block diagonal energy values
$\overline{E_{\mathrm{M}}}$: average of block energy values
$\overline{E_{\mathrm{S}}}$: standard deviation of block energy values

The T^2 statistic of a BDCT with five energy features of a testing image in the multivariate statistical model can be defined as (Montgomery, 2009):

$$T^2 = n\left(X_i - \overline{X_i}\right)^T S^{-1}\left(X_i - \overline{X_i}\right) \quad i = 1,\ 2,\ 3,\ ...,\ 5 \quad (10)$$

where *n* is the number of observations in a BDCT unit, X is the mean matrix of energy features in a BDCT unit of a testing image.

The control limits of the T^2 statistic are as follows:

$$UCL = \frac{p(m-1)}{m-p} F_{\theta,p,m-p}; \quad LCL = 0 \quad (11)$$

where *F* is a tabulated value of the *F* distribution at the significance level of θ Therefore, if a BDCT unit of a testing image has a higher T^2 value, it implies that the region contains defects in the testing image. On the contrary, a lower T^2 value signifies that no defect exist in the corresponding region of the image.

Grey clustering

The BDCT blocks with high T^2 values greater than the UCL are considered as the suspected defect blocks in a testing image. The grey clustering technique will be conducted to further confirm the block locations of real defects. The initial feature sequences of the suspected defect blocks can be presented as:

$$V = \left\{x_1,\ x_2,\ x_3,...,\ x_p\right\} \quad (12)$$

$$v_i = (E_H\ ,\ E_V\ ,\ E_D\ ,\ E_M\ ,\ E_S) \quad (13)$$

where *p* is the number of the suspected defect blocks detected by the T^2 statistic. The grey relational grade of the two sequences: Reference feature sequence v_i (*i* = 1, 2, 3, …, *p*) and comparative feature sequence v_j (*j* = 1, 2, 3, …, *p*) is defined as follows:

$$\gamma\left(v_i\ ,\ v_j\right) = \frac{1}{u}\sum_{k=1}^{u}\gamma\left(v_i(k), v_j(k)\right) \quad (14)$$

where *u* is the number of energy features, and

$$\gamma\left(v_i(k), v_j(k)\right) = \left(\frac{\Delta_{\max} - \Delta_{ij}(k)}{\Delta_{\max} - \Delta_{\min}}\right)^{\zeta} \quad (15)$$

where ζ is called distinguished coefficient and is set as 1 in this research, and

$$\Delta_{ij} = \left\|v_i(k) - v_j(k)\right\| \quad (16)$$

$$\Delta_{\max} = \max_{\forall k}\ \left\|v_i\ (k) - v_j(k)\right\| \quad (17)$$

$$\Delta_{\min} = \min_{\forall k}\left\|v_i\ (k) - v_j(k)\right\| \quad (18)$$

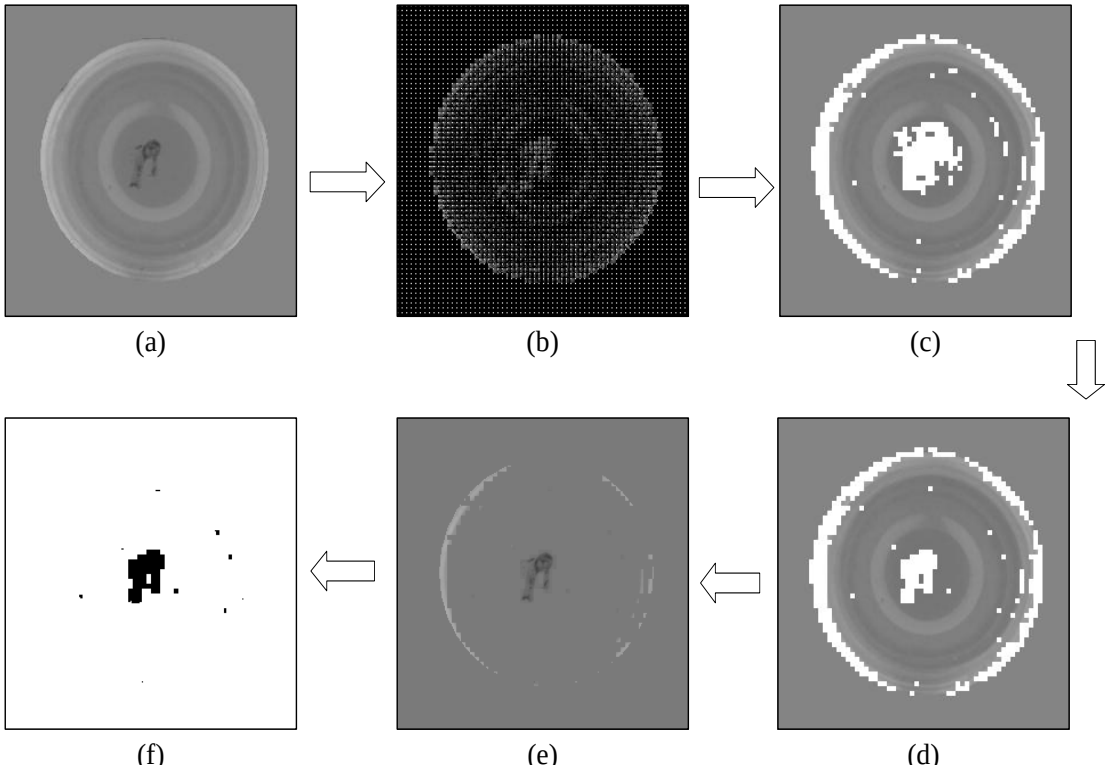

Figure 4. The proposed procedure of detecting visual defects on LED lens (a) a testing image; (b) the BDCT domain image; (c) the suspected defect blocks (in white) detected by T2 statistic; (d) the re-confirmed defect blocks by grey clustering; (e) the defect blocks with a manipulated background, and (f) resulting detected image.

The higher degree of relation means the comparative feature sequence is more similar to the reference feature sequence than the others. Using the grey relational measure to train the grey cluster among of the given data points, and clustering the data according to the grey relational grades. The updated feature sequence is calculated by the equation:

$$v_i^*(k) = \frac{\sum_{j=1}^{n} n_{ij} v_j(k)}{\sum_{j=1}^{n} n_{ij}}, \; k = 1, 2, \; 3, \; ..., \; 5 \tag{19}$$

where,

$$n_{ij} = \begin{cases} 1 & if \; \gamma_{ij} \geq \omega \\ 0 & if \; \gamma_{ij} < \omega \end{cases} \tag{20}$$

ω is a selected threshold with $0 < \omega < 1$. If all the updated feature sequences do not change (less than an allowance ε), the stop criterion of the iterations is:

$$\left| V_i - V_{i-1} \right| \leq \varepsilon \tag{21}$$

Finally, the convergent vector is viewed as the cluster center. The grey relational grades of the suspected defect blocks are calculated to further identify the block locations of real defects.

Figure 4 shows the results and differences performed the proposed method for detecting visual defects in LED lens. Figure 4b presents the BDCT domain image of Figure 4a. Figure 4c is the preliminary detected image with suspected defect blocks (in white) when the energy features are integrated by the T^2 statistic. Figure 4d depicts the primary detected image with defect blocks re-confirmed by the grey clustering technique. Figure 4e is a mixed image containing the detected defect blocks and a manipulated background for locating defect regions. Figure 4f is the resulting binary images that display the flaws in black by the proposed defect detection method. The results reveal that the visual flaws in LED lens are correctly segmented in the binary image, regardless of LED lens with transparent and curved surface.

RESULTS AND DISCUSSION

Implementation and analyses

Here, we implement the proposed approach and conduct experiments to evaluate its performance in detecting visual defects of LED lenses. To strengthen the visibility of the visual defects, we make use of the following equipments: a yellow ring lighting device, a USB 2.0 color

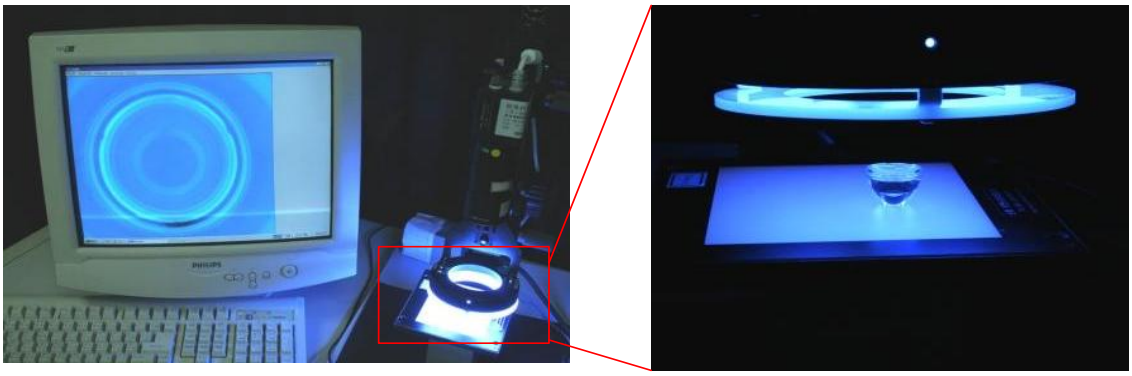

(a) (b)

Figure 5. Environmental configurations of scanning a testing LED lens sample: (a) Hardware setup of experiments; (b) a testing LED sample is placed on XY table.

CCD of ARTRAY company, a lens with 1 to 10 amplifications of changeable focal lengths, and a XYZ electronic control table with a controller. Experiments are conducted on 188 real LED lenses (including 128 normal lenses and 60 defective lenses) provided by a local manufacturing company of high quality LED lenses in Taiwan to evaluate the performance of the proposed approach. Figure 5 demonstrates the configurations of the environment in which we scan real LED lenses to be used as testing samples in the experiments. Each image of the LED lens has a size of 256 × 256 pixels and a gray level of 8 bits. The visual defect detection algorithm is edited in C language and executed on the 6th version of the C++ Builder complier on a personal computer (Pentium-4 2.8 GHz and 512 MB DDRII 667 Hz-RAM).

In industrial practice, when a detected blemish is larger than a pre-defined size, the inspection system alerts for the appearance of blemish. Sometimes, this information is not enough for quality control purpose because product quality measures not only the blemish volumes but also the blemish severity levels. The ranges of blemish sizes imply different severity levels of product blemishes. Thus, an inspection system should alert for the presence of blemishes, detect the blemish locations and calculate the blemish sizes in some applications. To verify the performance of the proposed method and traditional techniques, we compare the results of our experiments against those provided by professional inspectors by precisely matching the corresponding blemish locations and blemish sizes.

The performance evaluation indices, (1-α) and (1-β), are used to represent correct detection judgments; the higher the two indices, the more accurate the detection results. Statistical type I error α suggests the probability of producing false alarms, that is, detecting normal regions as defects. Statistical type II error β implies the probability of producing missing alarms, which fail to alarm real defects. We divide the area of normal region detected as defects by the area of actual normal region to obtain type I error, and the area of undetected defects by the area of actual defects to obtain type II error. The correct classification rate (CR) is defined as:

$$CR = (N_{cc} + N_{dd}) / N_{total} \times 100\% \quad (22)$$

where N_{cc} is the pixel number of normal textures detected as normal areas, N_{dd} is the pixel number of defects detected as defective regions, and N_{total} is the total pixel number of a testing image.

Figure 6 shows partial results of detecting visual defects by the Iterative method (Jain et al., 1995), the Otsu method (Otsu, 1979), Lin and Jiang (2007) method, the proposed method, and the professional inspector, individually. The two spatial domain techniques: the Iterative and Otsu methods, make lots of erroneous judgments (false alarms) on visual defect detection. The two frequency domain techniques, the Lin and Jiang approach and the proposed method, detect most of the visual blemishes and make less erroneous judgments. Therefore, the frequency domain approaches outperform the spatial domain techniques in the visual defect detection of LED lenses.

Table 1 summarizes the detection results of our experiments. Two spatial domain approaches and two frequency domain techniques are evaluated against the results by professional inspectors. The average defect detection rates *(1-β)* of all testing samples by the four methods are, respectively, 99.99% (Iterative method), 98.84% (Otsu method), 85.88% (Lin and Jiang method), and 94.64% (proposed method). However, the two spatial domain methods have significantly higher false alarm rates (α), 28.97% (Iterative method) and 30.03% (Otsu method). On the contrary, the other two frequency domain approaches have rather lower false alarm rates, 0.008% (Lin and Jiang method) and 0.15% (proposed method).

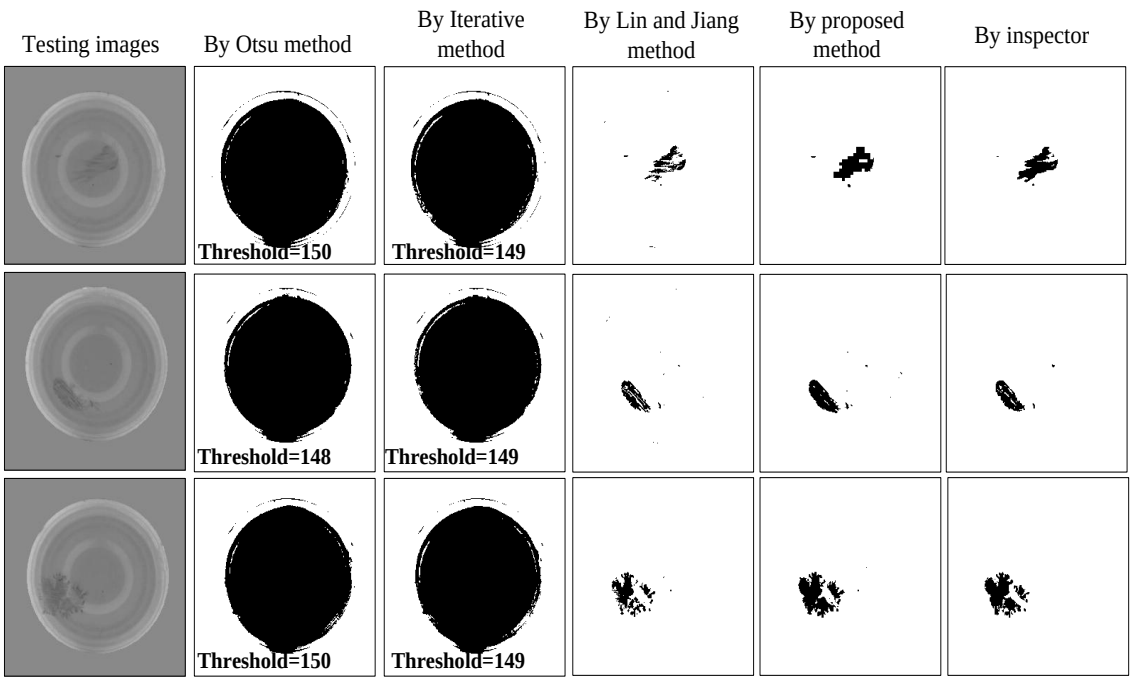

Figure 6. Partial detection results of the Otsu, Iterative, Lin and Jiang, the proposed methods, and inspector.

Table 1. Summarized comparison table of visual defect detection of LED lenses for four different methods.

Comparison characteristics	Spatial domain approaches		Frequency domain approaches	
	Otsu method	Iterative method	Lin and Jiang method	Proposed method
1-β (%)	98.84	99.99	85.88	94.64
α (%)	30.03	28.97	0.008	0.15
CR (%)	70.26	71.37	99.6	99.67
Time (s)	0.6	0.5	0.7	0.27

The proposed method has higher correct classification rates (CR) than do the other methods applied to defect detection of LED lens images. More specifically, the proposed method not only has a higher detection rate than does the Lin and Jiang method but also its false alarm rate is more than eighteeen times lower than that of the latter method applied to LED lens images.

The average computation time for processing an image of 256 × 256 pixels is as follows: 0.6 s by the Otsu method, 0.5 s by the Iterative method, 0.7 s by the Lin and Jiang method, and 0.27 s by the proposed method. The average processing time of the proposed method is more than two times shorter than that of the Lin and Jiang method. The proposed method overcomes the difficulties of detecting visual blemishes on LED lens images with curved surfaces and excels in its ability of correctly discriminating visual blemishes from normal regions.

Conclusions

Machine vision technology improves productivity and quality management, and provides a competitive advantage to industries that employ this technology. This research proposes a novel approach that applies block discrete cosine transform, Hotelling T^2 statistic, and grey clustering technique for the automatic inspection of visual defects in curved surfaces of LED lenses. Real LED lenses are used as testing samples, and large-sample experiments are conducted in a real inspection environment to verify the performance of the proposed approach. Experimental results show that the proposed approach achieves a high 94.64% probability of correctly discriminating visual defects from normal regions and a low 0.15% probability of erroneously detecting normal regions as defects on curved surfaces of LED lenses. Compared with other traditional methods, this approach

has the advantages of higher detection rates, lower false alarm rates, and shorter average processing time. This method not only overcomes the difficulties of inspecting visual defects on curved surfaces but also relies on no template matching process.

The proposed method is based on feature extraction from BDCT-domain images for defect detection. Since the computation of multivariate statistic is based on the mean vector and covariance matrix of training samples, the lighting changes may lead to the increase of variation in statistics and result in affecting the effect of defect detection. It is recommended to re-compute the mean vector and covariance of the training samples when illumination is significantly changed. Future research may extend the proposed method to similar low-contrast defect detection problems, such as abnormal inspection of medical images and tiny defect detections of electronic and optical components. This research contributes a solution to a common surface defect detection problem of LED lenses and offers a computer-aided visual defect inspection system to meet the inspection and quality control request.

ACKNOWLEDGEMENT

This work was partially supported by the National Science Council (NSC) of Taiwan, under Grant No. NSC 97-2221-E-324-020-MY3.

Nomenclature: $d_{x,y}$, a digital image with coordinate (x, y) in spatial domain; $D_{u,v}$, a digital image with coordinate (u, v) in discrete cosine transform domain; $P(u, v)$, the power spectrum of image $D_{u, v}$; E_H, the horizontal energy value of a BDCT; E_V, the vertical energy value of a BDCT; E_D, the diagonal energy value of a BDCT; E_M, the average energy value of a BDCT; E_S, the standard deviation of energy values of a BDCT; S, the sample covariance matrix of a normal image; $\bar{X}$, the sample mean matrix of a normal image; T^2, a statistic of a BDCT with five energy features of a testing image in the multivariate statistical model; UCL, the upper control limit of the T^2 statistic; LCL, the lower control limit of the T^2 statistic; V, the initial feature sequences of the suspected defect blocks; $\gamma(v_i, v_j)$, the grey relational grade of the reference feature sequence v_i and the comparative feature sequence v_j; $v_i(k)$, the reference feature sequence of the i-th suspected defect block with k energy values; CR, the correct classification rate of a defect detection method.

REFERENCES

Ahmed N, Natarajan T, Rao KR (1974). Discrete cosine transform. IEEE Trans. Comput., 23: 90-93.

Bazin AI, Cole T, Kett B, Nixon MS (2006). An automated system for contact lens inspection. Lect. Notes Comput. Sci., 4291: 141-150.

Chan CH, Pang GKH (2000). Fabric defect detection by Fourier analysis. IEEE Trans. Ind. Appl., 36: 1267-1276.

Cho CS, Chung BM, Park MJ (2005). Development of real-time vision-based fabric inspection system. IEEE Trans. Ind. Electron., 52: 1073-1079.

Deng JL (1989). Introduction to grey system theory. J. Grey Syst., 1: 1-24.

Gonzalez RC, Woods RE (2008). Digital Image Processing. 3rd Ed., Prentice Hall, New Jersey, USA.

Heng Z (2010). Analysis of infrared images based on grey system and neural network. Kybern., 39(8): 1366-1375.

Hu YC, Chen RS, Hsu YT, Tzeng GH (2002). Grey self-organizing feature maps. Neurocom., 48: 863-877.

Huang KY (2008). An auto-recognizing system for dice games using a modified unsupervised grey clustering algorithm. Sensors, 8: 1212-1221.

Jain R, Kasturi R, Schunck BG (1995). Machine Vision. International Editions, McGraw Hill, New York, NY, USA.

Latif-Amet A, Ertüzün A, Ercil A (2000). An efficient method for texture defect detection: sub-band domain co-occurrence matrices. Image Vision Comput., 18: 543-553.

Lin CH, Wu CH, Huang PZ (2009). Grey clustering analysis for incipient fault diagnosis in oil-immersed transformers. Expert Syst. Appl., 36: 1371-1379.

Lin HD, Ho DC (2007). Detection of pinhole defects on chips and wafers using DCT enhancement in computer vision systems. Int. J. Adv. Manuf. Technol., 34(5-6): 567-583.

Lin HD, Jiang JD (2007). Applying discrete cosine transform and grey relational analysis to surface defect detection of LED. J. Chin. Inst. Ind. Eng., 24(6): 458-467.

Lin YH, Lee PC (2009). Effective evaluation model under the condition of insufficient and uncertain information. Expert Syst. Appl., 36: 5600-5604.

Martínez SS, Ortega JG, García JG, García AS (2009). A sensor planning system for automated headlamp lens inspection. Expert Syst. Appl., 36: 8768-8777.

Madhuri B, Chandulal J (2010). Evaluating web sites using COPRAS GRA combined with grey clustering. Int. J. Eng. Sci. Technol., 2(10): 5280-5294.

Montgomery DC, Runger GC (2007). Applied Statistics and Probability for Engineers. 4th Edition, John Wiley & Sons, New Jersey, USA.

Montgomery DC (2009). Statistical Quality Control: A Modern Introduction. 6th Edition, John Wiley & Sons, New York, NY, USA.

Otsu N (1979). A threshold selection method from gray level histogram. IEEE Trans. Syst. Man Cybern. Part B Cybern., 9: 62-66.

Pan F (2002). Adaptive image compression using local pattern information. Patt. Recognit. Lett., 23(14): 1837-1845.

Perng DB, Wang WC, Chen SH (2010). A novel quasi-contact lens auto-inspection system. J. Chin. Inst. Ind. Eng., 27(4): 260-269.

Rao KR, Hwang JJ (1996). Techniques and Standards for Image, Video and Audio Coding. Prentice Hall PTR, New Jersey, USA.

Rebsamen M, Boucheix JM, Fayol M (2010). Quality control in the optical industry: From a work analysis of lens inspection to a training programme, an experimental case study. Appl. Ergon., 41: 150-160.

Tsai DM, Hsiao B (2001). Automatic surface inspection using wavelet reconstruction. Patt. Recognit., 34: 1285-1305.

Tsai HC, Hsiao SW, Hung FK (2006). An image evaluation approach for parameter-based product form and color design. Comput.-Aided Des,. 38: 157-171.